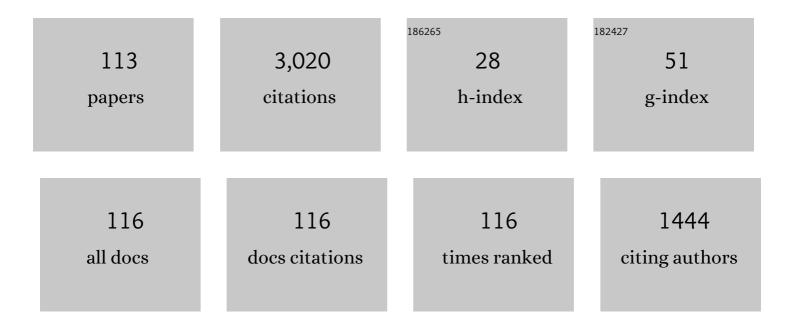
List of Publications by Year in descending order

Source: https://exaly.com/author-pdf/3385412/publications.pdf Version: 2024-02-01



#	Article	IF	CITATIONS
1	lonospheric effects of major magnetic storms during the International Space Weather Period of September and October 1999: GPS observations, VHF/UHF scintillations, and in situ density structures at middle and equatorial latitudes. Journal of Geophysical Research, 2001, 106, 30389-30413.	3.3	204
2	Response of the equatorial ionosphere in the South Atlantic Region to the Great Magnetic Storm of July 15, 2000. Geophysical Research Letters, 2001, 28, 3577-3580.	4.0	202
3	Equatorial scintillation and systems support. Radio Science, 1997, 32, 2047-2064.	1.6	188
4	Response of the equatorial ionosphere at dusk to penetration electric fields during intense magnetic storms. Journal of Geophysical Research, 2007, 112, .	3.3	122
5	Radar observations of the onset of current driven instabilities in the topside ionosphere. Geophysical Research Letters, 1988, 15, 160-163.	4.0	91
6	Conjugate Point Equatorial Experiment (COPEX) campaign in Brazil: Electrodynamics highlights on spread <i>F</i> development conditions and dayâ€ŧoâ€day variability. Journal of Geophysical Research, 2009, 114, .	3.3	90
7	Postmidnight bubbles and scintillations in the quietâ€time June solstice. Geophysical Research Letters, 2013, 40, 5592-5597.	4.0	85
8	Global equatorial plasma bubble occurrence during the 2015 St. Patrick's Day storm. Journal of Geophysical Research: Space Physics, 2016, 121, 894-905.	2.4	78
9	Simulating the impacts of ionospheric scintillation on L band SAR image formation. Radio Science, 2012, 47, .	1.6	77
10	Dynamics of equatorialFregion irregularities from spaced receiver scintillation observations. Geophysical Research Letters, 2001, 28, 119-122.	4.0	75
11	Equatorial plasma bubbles and L-band scintillations in Africa during solar minimum. Annales Geophysicae, 2012, 30, 675-682.	1.6	75
12	Measurement of the latitudinal distributions of total electron content during equatorial spreadFevents. Journal of Geophysical Research, 2001, 106, 29133-29152.	3.3	70
13	Near-simultaneous plasma structuring in the midlatitude and equatorial ionosphere during magnetic superstorms. Geophysical Research Letters, 2005, 32, n/a-n/a.	4.0	68
14	Ground and Space-Based Measurement of Rocket Engine Burns in the Ionosphere. IEEE Transactions on Plasma Science, 2012, 40, 1267-1286.	1.3	58
15	On the Relationship Between the Rate of Change of Total Electron Content Index (ROTI), Irregularity Strength (<i>C</i> _{<i>k</i>} <i>L</i>), and the Scintillation Index (<i>S</i> _{<i>4</i>}). Journal of Geophysical Research: Space Physics, 2019, 124, 2099-2112.	2.4	56
16	Stimulated Brillouin Scatter in a Magnetized Ionospheric Plasma. Physical Review Letters, 2010, 104, 165004.	7.8	55
17	Geomagnetic control of equatorial plasma bubble activity modeled by the TIEGCM with <i>Kp</i> . Geophysical Research Letters, 2014, 41, 5331-5339.	4.0	55
18	Dayâ€ŧoâ€day variability of the equatorial ionization anomaly and scintillations at dusk observed by GUVI and modeling by SAMI3. Journal of Geophysical Research, 2009, 114, .	3.3	54

#	Article	IF	CITATIONS
19	Longitudinal and Seasonal Variability of Equatorial Ionospheric Irregularities and Electrodynamics. Space Weather, 2018, 16, 946-968.	3.7	50
20	Specification of the occurrence of equatorial ionospheric scintillations during the main phase of large magnetic storms within solar cycle 23. Radio Science, 2010, 45, n/a-n/a.	1.6	46
21	Equatorial plasma depletion precursor signatures and onset observed at 11° south of the magnetic equator. Journal of Geophysical Research, 1996, 101, 26829-26838.	3.3	45
22	Impacts of ionospheric scintillations on GPS receivers intended for equatorial aviation applications. Radio Science, 2012, 47, .	1.6	44
23	Validation of the NeQuick 2 and IRI-2007 models in East-African equatorial region. Journal of Atmospheric and Solar-Terrestrial Physics, 2013, 102, 26-33.	1.6	44
24	lonospheric scintillation monitoring and mitigation using a software GPS receiver. Radio Science, 2004, 39, n/a-n/a.	1.6	43
25	Multiple phase screen modeling of ionospheric scintillation along radio occultation raypaths. Radio Science, 2011, 46, .	1.6	43
26	L-band scintillation activity and space-time structure of low-latitude UHF scintillations. Radio Science, 2003, 38, 4-1-4-9.	1.6	42
27	Effect of magnetic activity on the dynamics of equatorialFregion irregularities. Journal of Geophysical Research, 2002, 107, SIA 20-1-SIA 20-7.	3.3	40
28	Latitudinal and Local Time Variation of Ionospheric Turbulence Parameters during the Conjugate Point Equatorial Experiment in Brazil. International Journal of Geophysics, 2012, 2012, 1-16.	1.1	30
29	Kalman filter estimation of plasmaspheric total electron content using GPS. Radio Science, 2009, 44, .	1.6	28
30	A physicsâ€based model for the ionization of samarium by the MOSC chemical releases in the upper atmosphere. Radio Science, 2017, 52, 559-577.	1.6	27
31	Signal distortion on VHF/UHF transionospheric paths: First results from the Wideband Ionospheric Distortion Experiment. Radio Science, 2006, 41, .	1.6	25
32	Magnetic conjugate point observations of kilometer and hundredâ€meter scale irregularities and zonal drifts. Journal of Geophysical Research, 2010, 115, .	3.3	25
33	Correlation of in situ measurements of plasma irregularities with groundâ€based scintillation observations. Journal of Geophysical Research, 2010, 115, .	3.3	24
34	Using solar wind data to predict daily GPS scintillation occurrence in the African and Asian Iow″atitude regions. Geophysical Research Letters, 2014, 41, 8176-8184.	4.0	24
35	Coordinated study of coherent radar backscatter and optical airglow depletions in the central Pacific. Journal of Geophysical Research, 2010, 115, .	3.3	23
36	Equatorial scintillation calculations based on coherent scatter radar and C/NOFS data. Radio Science, 2011, 46, .	1.6	23

#	Article	IF	CITATIONS
37	Artificial ionospheric modification: The Metal Oxide Space Cloud experiment. Radio Science, 2017, 52, 539-558.	1.6	23
38	A comprehensive rocket and radar study of midlatitude spread <i>F</i> . Journal of Geophysical Research, 2010, 115, .	3.3	22
39	Leveraging Geodetic GPS Receivers for Ionospheric Scintillation Science. Radio Science, 2020, 55, e2020RS007131.	1.6	21
40	Measurements of artificial periodic inhomogeneities at HIPAS Observatory. Journal of Geophysical Research, 1997, 102, 24023-24035.	3.3	20
41	A regional GPS receiver network for monitoring equatorial scintillation and total electron content. Radio Science, 2001, 36, 1545-1557.	1.6	20
42	Ionospheric scintillation effects on single frequency GPS. Space Weather, 2008, 6, .	3.7	20
43	Threeâ€dimensional numerical simulations of equatorial spread <i>F</i> : Results and observations in the Pacific sector. Journal of Geophysical Research, 2012, 117, .	3.3	20
44	Specification and Forecasting of Outages on Satellite Communication and Navigation Systems. Geophysical Monograph Series, 0, , 423-430.	0.1	19
45	Climatology of GPS amplitude scintillations over equatorial Africa during the minimum and ascending phases of solar cycle 24. Astrophysics and Space Science, 2015, 357, 1.	1.4	19
46	A characterization of intermediateâ€scale spread <i>F</i> structure from fourÂyears of highâ€resolution C/NOFS satellite data. Radio Science, 2016, 51, 779-788.	1.6	19
47	Evolution of Mid″atitude Density Irregularities and Scintillation in North America During the 7–8 September 2017 Storm. Journal of Geophysical Research: Space Physics, 2021, 126, e2021JA029192.	2.4	19
48	Validation of WBMOD in the Southeast Asian region. Radio Science, 2001, 36, 1559-1572.	1.6	18
49	C/NOFS satellite observations of equatorial ionospheric plasma structures supported by multiple ground-based diagnostics in October 2008. Journal of Geophysical Research, 2011, 116, n/a-n/a.	3.3	18
50	Signature of the coronal hole near the north crest equatorial anomaly over Egypt during the strong geomagnetic storm 5 April 2010. Journal of Geophysical Research, 2012, 117, .	3.3	17
51	A technique for inferring zonal irregularity drift from singleâ€station GNSS measurements of intensity (<i>S</i> ₄) and phase (<i>Ïf</i> _φ) scintillations. Radio Science, 2016, 51, 1263-1277.	1.6	17
52	Stimulated thermal instability for ELF and VLF wave generation in the polar electrojet. Geophysical Research Letters, 2000, 27, 85-88.	4.0	15
53	GPS proxy model for real-time UHF satellite communications scintillation maps from the Scintillation Network Decision Aid (SCINDA). Radio Science, 2004, 39, n/a-n/a.	1.6	15
54	On the Assessment of Daily Equatorial Plasma Bubble Occurrence Modeling and Forecasting. Space Weather, 2020, 18, e2020SW002555.	3.7	15

#	Article	IF	CITATIONS
55	Suprathermal electrons generated by the interaction of powerful radio wave with the ionosphere. Geophysical Research Letters, 2000, 27, 2461-2464.	4.0	14
56	Performance of 6 Different Global Navigation Satellite System Receivers at Low Latitude Under Moderate and Strong Scintillation. Earth and Space Science, 2021, 8, e2020EA001314.	2.6	14
57	Using ionospheric scintillation observations for studying the morphology of equatorial ionospheric bubbles. Radio Science, 2004, 39, n/a-n/a.	1.6	13
58	Signatures of equatorial plasma bubbles in VHF satellite scintillations and equatorial ionograms. Radio Science, 2013, 48, 89-101.	1.6	13
59	The electrodynamic effects of MOSCâ€like plasma clouds. Radio Science, 2017, 52, 604-615.	1.6	13
60	A combined spectroscopic and plasma chemical kinetic analysis of ionospheric samarium releases. Radio Science, 2017, 52, 521-538.	1.6	13
61	Empirical modeling of plasma clouds produced by the Metal Oxide Space Clouds experiment. Radio Science, 2017, 52, 578-596.	1.6	13
62	Unseasonal development of post-sunset F-region irregularities over Southeast Asia on 28 July 2014: 1. Forcing from above?. Progress in Earth and Planetary Science, 2018, 5, .	3.0	13
63	Spatial Spectrum of Artificial Ionospheric Irregularities Induced by Powerful HF Radiowaves. Radiophysics and Quantum Electronics, 2001, 44, 833-846.	0.5	12
64	Operational Space Environment Network Display (OpSEND). Radio Science, 2004, 39, n/a-n/a.	1.6	12
65	Longitudinal correlation of equatorial ionospheric scintillation. Radio Science, 2006, 41, .	1.6	12
66	Simulating the effects of scintillation on transionospheric signals with a twoâ€way phase screen constructed from ALTAIR phaseâ€derived TEC. Radio Science, 2009, 44, .	1.6	12
67	Ionospheric Es layer scintillation characteristics studied with Hilbert-Huang transform. Advances in Space Research, 2019, 64, 2137-2144.	2.6	12
68	Laboratory reproduction of arecibo experimental results: HF wave-enhanced Langmuir waves. Geophysical Research Letters, 1997, 24, 115-118.	4.0	11
69	Study of large-scale irregularities generated in the ionosphericF-region by high-power HF waves. Radiophysics and Quantum Electronics, 2000, 43, 446-468.	0.5	11
70	Extreme longitudinal variability of plasma structuring in the equatorial ionosphere on a magnetically quiet equinoctial day. Radio Science, 2006, 41, n/a-n/a.	1.6	9
71	A phase screen simulator for predicting the impact of small-scale ionospheric structure on SAR image formation and interferometry. , 2010, , .		9
72	The effect of phase scintillations on the accuracy of phase screen simulation using deterministic screens derived from GPS and ALTAIR measurements. Radio Science, 2012, 47, .	1.6	9

#	Article	IF	CITATIONS
73	HF propagation results from the Metal Oxide Space Cloud (MOSC) experiment. Radio Science, 2017, 52, 710-722.	1.6	9
74	Seasonal modulation of GPS performance due to equatorial scintillation. Geophysical Research Letters, 2004, 31, .	4.0	8
75	lonosphericâ€ŧhermospheric UV tomography: 2. Comparison with incoherent scatter radar measurements. Radio Science, 2017, 52, 357-366.	1.6	8
76	Wave-Optics Analysis of HF Propagation through Traveling Ionospheric Disturbances and Developing Plasma Bubbles. , 2020, , .		8
77	Ionospheric effects on GPS signals in the Arctic region using early GPS data from Thule, Greenland. Radio Science, 2009, 44, n/a-n/a.	1.6	7
78	TEC variations during geomagnetic storm/substorm with Pc5/Pl2 pulsation signature. Advances in Space Research, 2015, 55, 2534-2542.	2.6	7
79	Unseasonal development of post-sunset F-region irregularities over Southeast Asia on 28 July 2014: 2. Forcing from below?. Progress in Earth and Planetary Science, 2018, 5, .	3.0	7
80	A Comparison of Electron Densities Derived by Tomographic Inversion of the 135.6â€nm Ionospheric Nightglow Emission to Incoherent Scatter Radar Measurements. Journal of Geophysical Research: Space Physics, 2019, 124, 4585-4596.	2.4	7
81	Radar Investigation of Postsunset Equatorial Ionospheric Instability Over Kwajalein During Project WINDY. Journal of Geophysical Research: Space Physics, 2020, 125, e2020JA027997.	2.4	7
82	Modeling the low-latitude ionospheric electron density and plasma turbulence in the November 2004 storm period. Journal of Atmospheric and Solar-Terrestrial Physics, 2010, 72, 350-357.	1.6	6
83	A Configuration Space Model for Intermediateâ€Scale Ionospheric Structure. Radio Science, 2018, 53, 1472-1480.	1.6	6
84	Forcing From Lower Thermosphere and Quiet Time Scintillation Longitudinal Dependence. Space Weather, 2020, 18, e2020SW002610.	3.7	6
85	International Heliophysical Year: GPS Network in Africa. Earth, Moon and Planets, 2009, 104, 263-270.	0.6	5
86	In situ irregularity identification and scintillation estimation using wavelets and CINDI on C/NOFS. Radio Science, 2013, 48, 388-395.	1.6	5
87	Preliminary HF results from the Metal Oxide Space Cloud (MOSC) experiment. , 2014, , .		5
88	On the Nature of the Intraseasonal Variability of Nighttime Ionospheric Irregularities Over Taiwan. Journal of Geophysical Research: Space Physics, 2019, 124, 3609-3622.	2.4	5
89	VHF Scintillation and Drift Studied Using Spaced Receivers in Southern Taiwan. Radio Science, 2019, 54, 455-467.	1.6	5
90	Wave Field Propagation in Extended Highly Anisotropic Media. Radio Science, 2019, 54, 646.	1.6	4

#	Article	IF	CITATIONS
91	Detection of Ionospheric Structures with L-Band Synthetic Aperture Radars. , 2008, , .		3
92	Equatorial scintillation predictions from C/NOFS Planar Langmuir Probe electron density fluctuation data. , 2011, , .		3
93	lonosphericâ€thermospheric UV tomography: 3. A multisensor technique for creating fullâ€orbit reconstructions of atmospheric UV emission. Radio Science, 2017, 52, 896-916.	1.6	3
94	Statistics of Durations and Spacings of Equatorial Plasma Depletions Detected by the C/NOFS Planar Langmuir Probe. Space Weather, 2018, 16, 870-886.	3.7	3
95	The effect of ionospheric scintillation on phase gradient autofocus processing of synthetic aperture radar. , 2011, , .		2
96	Digital signal processing for ionospheric propagation diagnostics. Radio Science, 2015, 50, 837-851.	1.6	2
97	On the Generation of an Unseasonal EPB Over South East Asia. Journal of Geophysical Research: Space Physics, 2021, 126, e2020JA028724.	2.4	2
98	A Statistical Comparison of Satellite Tracking Performances During Ionospheric Scintillation for the GNSS Constellations GPS, Galileo and GLONASS. , 0, , .		2
99	lonosar - collaborative research towards understanding and mitigating ionospheric effects in SAR. , 2012, , .		1
100	A propagation model for geolocating ionospheric irregularities along radio occultation ray-paths. , 2017, , .		1
101	Combined operation of two ground transmitters for enhanced ionospheric heating Journal of Geomagnetism and Geoelectricity, 1988, 40, 1141-1145.	0.9	1
102	A Study of Postâ€Sunset Spreadâ€F Initiation During the 2013 EVEX Campaign. Journal of Geophysical Research: Space Physics, 2022, 127, .	2.4	1
103	Artificial ionospheric cavity induced by the radiation from the "sura―facility. Radiophysics and Quantum Electronics, 1999, 42, 601-608.	0.5	Ο
104	Use of real-time ionospheric scintillation data from multiple stations for nowcasting equatorial ionospheric bubble activity. , 2001, , .		0
105	C/NOFS: a demonstration system to forecast equatorial ionospheric scintillation that adversely affects navigation, communication, and surveillance systems. , 2004, 5548, 358.		Ο
106	MF/HF/VHF Radar Observations of Polar Mesosphere Summer Echoes (PMSE). IEEE National Radar Conference - Proceedings, 2007, , .	0.0	0
107	Study of the ionospheric scintillation and TEC characteristics at solar minimum in a West African equatorial region using Global Positioning System (GPS) data. , 2011, , .		0
108	Equatorial scintillation characteristics during solar minimum: Observations from the SCINDA network. , 2011, , .		0

7

#	Article	IF	CITATIONS
109	An inverse diffraction method for mapping the deterministic structure of ionospheric scintillations from one frequency to another. , 2014, , .		0
110	Simulating ionograms by compounding optically observed plasma clouds with ionospheric modelling technology. , 2015, , .		0
111	A new assimilative model for intermediate scale ionospheric structure. , 2015, , .		0
112	3D Multiâ€fluid MHD Simulation of the Early Time Behavior of an Artificial Plasma Cloud in the Bottom Side Ionosphere. Journal of Geophysical Research: Space Physics, 2021, 126, e2020JA029036.	2.4	0
113	Quantitative Scintillation Diagnostics Using Total Electron Content from Commercial Off-The-Shelf GNSS Receivers. , 0, , .		0